Supporting Information

Probing Single-chain Conformation and Its Impact on Optoelectronic Properties of Donor-Accepter Conjugated Polymers

Zhiqiang Cao,[a]† Zhaofan Li,[b]† Sara A. Tolba,[b] Gage T. Mason,[c] Miao Xiong,[d] Michael U. Ocheje,[c] Amirhadi Alesadi,[b] Changwoo Do,[e] Kunlun Hong,[f] Ting Lei,[d] Simon Rondeau-Gagné,[c] Wenjie Xia,[*b] Xiaodan Gu[*a]

a. School of Polymer Science and Engineering, The University of Southern Mississippi, Hattiesburg, MS 39406, USA. E-mail: xiaodan.gu@usm.edu
b. Department of Civil, Construction, and Environmental Engineering, North Dakota State University, Fargo, ND 58108, USA. E-mail: wenjie.xia@ndsu.edu
c. Department of Chemistry and Biochemistry, Advanced Materials Centre of Research (AMCORe), University of Windsor, Windsor, Ontario, N9B3P4, Canada.
d. School of Material Science and Engineering, Peking University, Beijing 100871, China.
e. Neutron Scattering Division, Oak Ridge National Laboratory, Oak Ridge, TN 37831, USA.
f. Center for Nanophase Materials Sciences, Oak Ridge National Laboratory, Oak Ridge, TN 37831, USA.

† These authors contributed equally to this work.

[*]Corresponding authors. E-mail address: xiaodan.gu@usm.edu; wenjie.xia@ndsu.edu

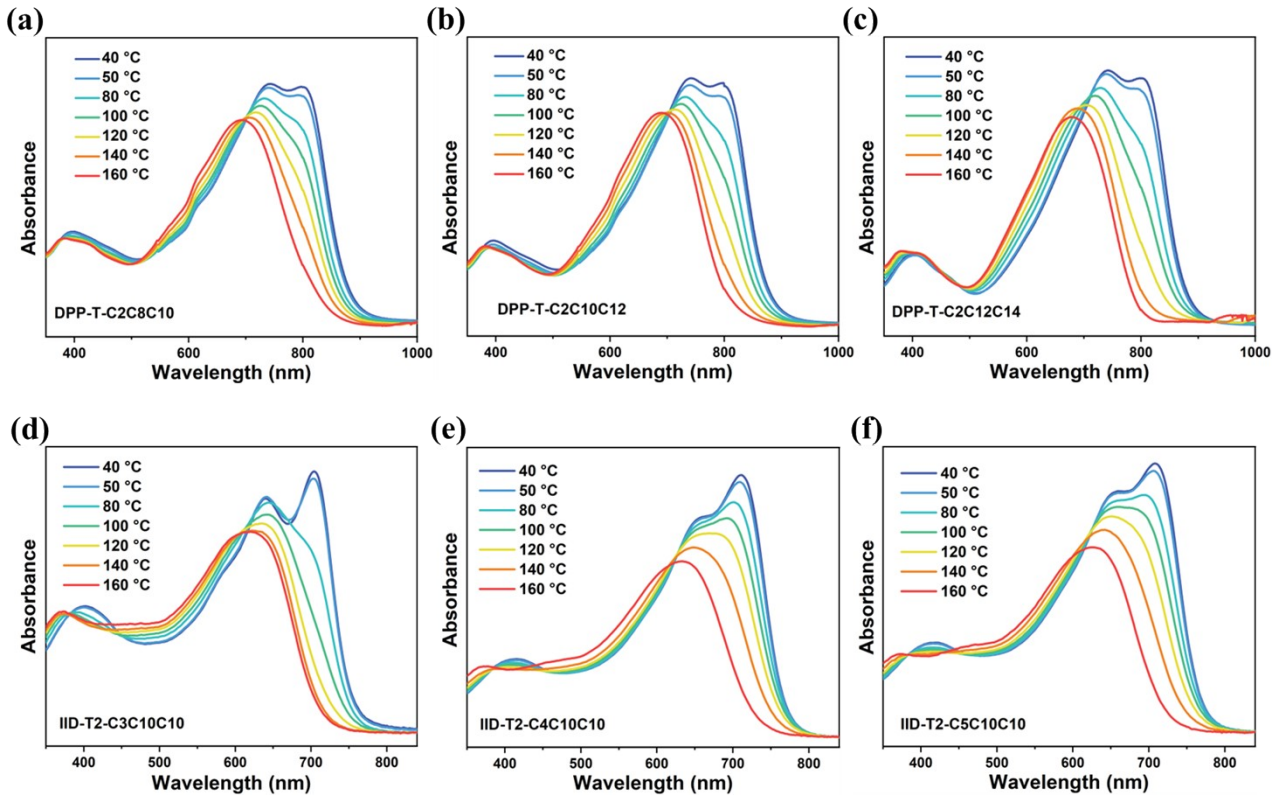

Figure S1. Temperature-dependent UV-vis for DPP-based and IID-based polymer solution in *o*-DCB. (0.1 mg/ml)

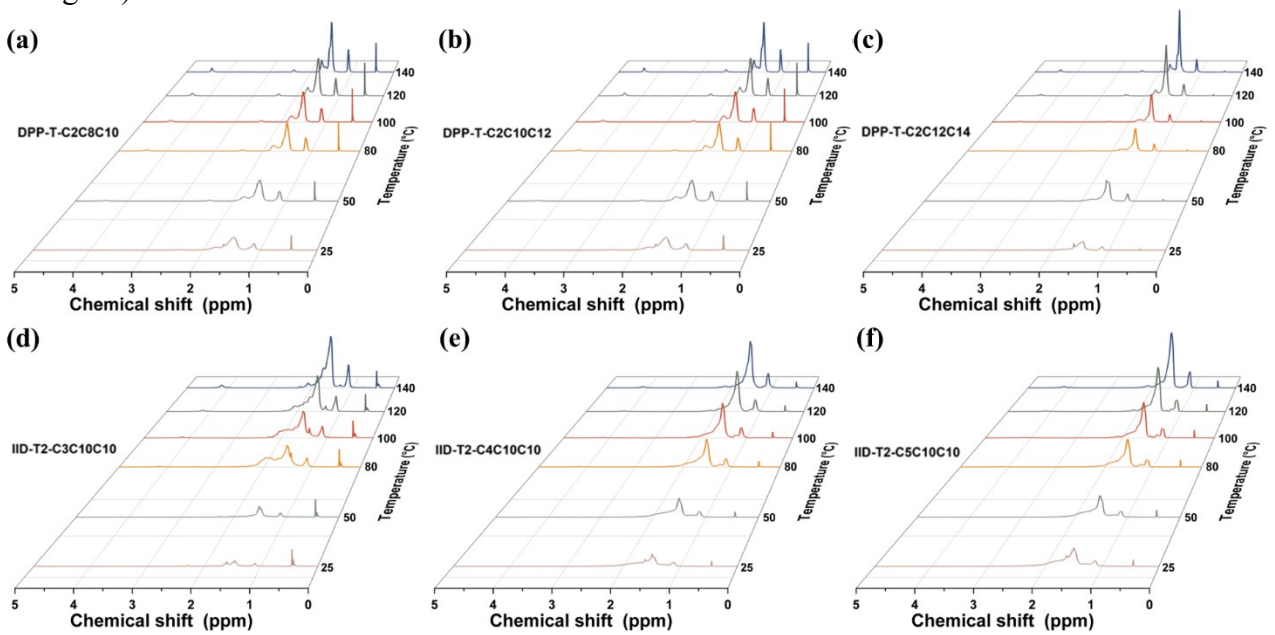

Figure S2. ^{1}H NMR spectra of DPP-based and IID-based polymer solution in *o*-DCB-d4 (5 mg/ml).

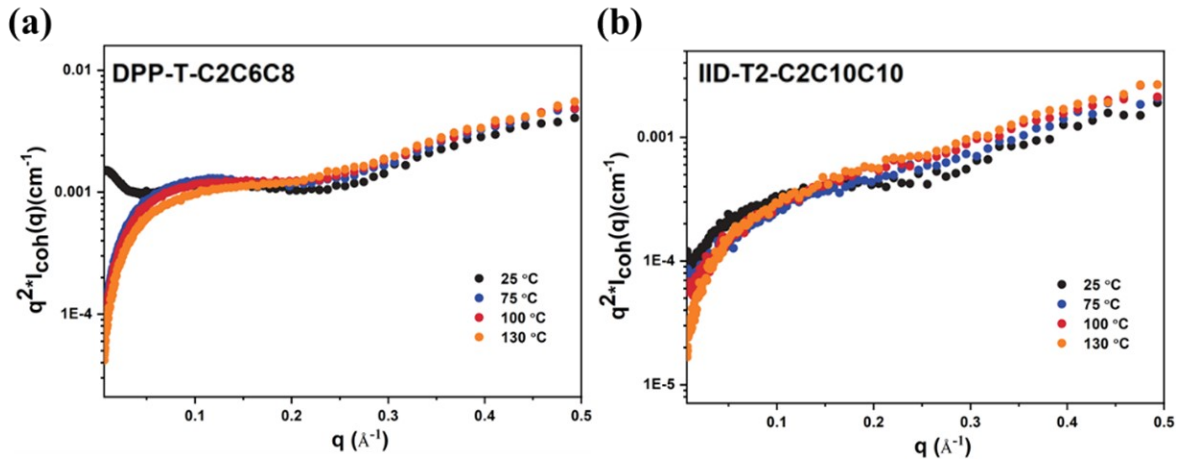

Figure S3. Kratky plots for (a) DPP-T-C2C6C8 and (b) IID-T2-C2C10C10.

For SANS curves measured below 130 °C, we used a combined model of flexible cylinder model (for single chains) and parallelepiped model:

$$I(q) = A_1 K_{para}^{2} P_{para}(A,B,C,q) + A_2 K_{cyl}^{2} P_{cyl}(L_c,l_p,R,q) + Background \quad (1)$$

in which A_1, A_2 are the scaling factors corresponding to the volume fraction of the particles; K_{cyl} and K_{papa} are the scattering contrast; A, B, C are the thickness, width, and length of the parallelepiped; L_c,l_p,R is the contour length, persistence length and radius of the flexible cylinder, respectively.

Persistence length calculation in MD

We performed the persistence length l_p calculation by considering the center-of-mass of consecutive functional groups (*i.e.*, DPP-core and thiophene ring for DPP based polymers, and isoindigo unit and thiophene ring for IID based polymers) along the backbone chain contour. $\mathbf{v}_s$ was denoted as the tangent vector connecting two segments *s* and *s*+1, and the l_p was determined from the tangent-tangent correlation function $\langle \mathbf{v}_0 \cdot \mathbf{v}_s \rangle$ with the average taken over all trajectories[1,2]:

$$\langle v_0 \cdot v_s \rangle = e^{-s/n_p} \quad (2)$$

where n_p is the persistence length measured in the number of monomers. l_p is taken as $l_p = l_0 n_p$, in which l_0 is the average monomer repeat unit length.

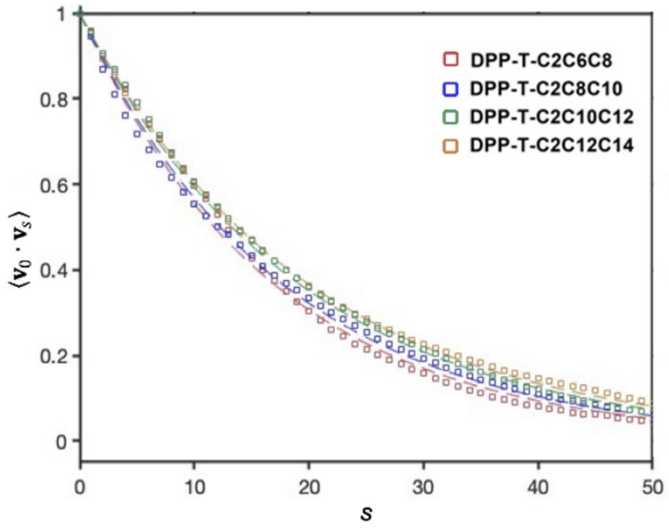

Figure S4. The l_p was determined from the tangent-tangent correlation function.

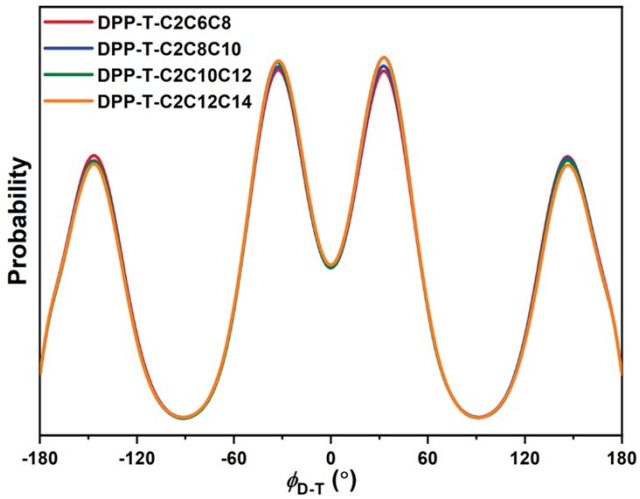

Figure S5. DPP-thiophene dihedral angle distributions from AA-MD simulation.

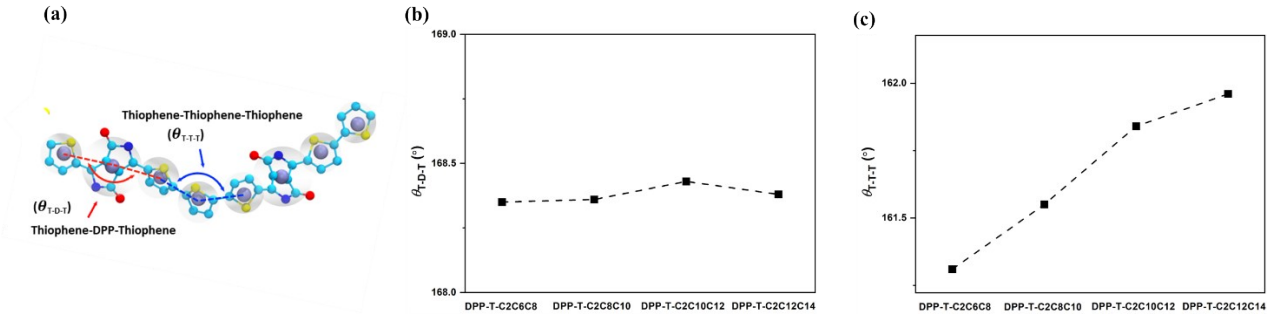

Figure S6. (a) Schematic definition of the bending angle. Grey beads denote the center of mass of each functional group. (b) Averaged bending angle between DPP-thiophene rings. (b) Averaged bending angle between thiophene-thiophene rings.

Furthermore, we also studied the averaged bending angles along the backbone chain, as measured by the angle formed by three consecutive center-of-mass of functional groups, including θ_{T-T-T} and θ_{T-D-T} (as labeled in **Figure 6c**). An increased averaged bending angle θ_{T-T-T} has been found with increasing side-chain length (**Figure 6e**), indicating that the growth of the side-chain length favors less bending and leads to more planar conformations of the polymer backbone.

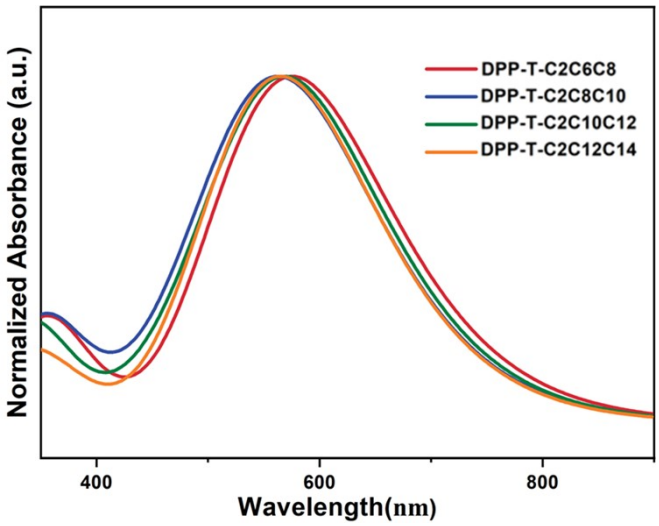

Figure S7. DFT calculated optical absorption based on the optimized ground-state electronic structure of DPP dimers.

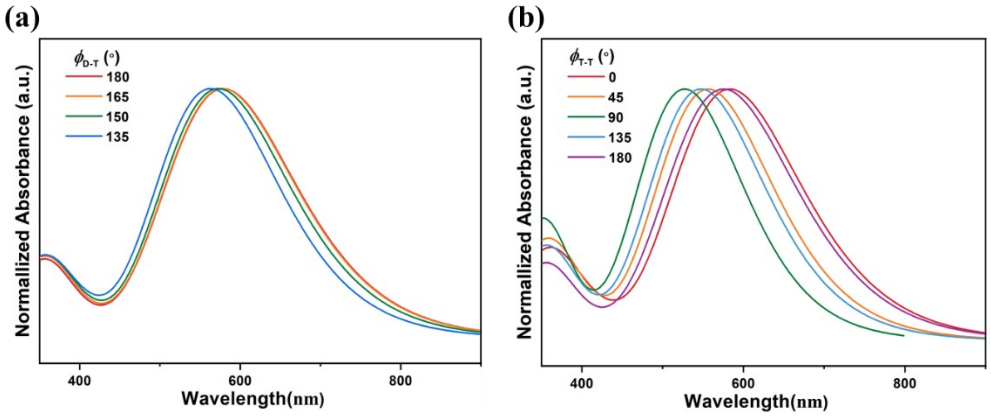

Figure S8. DFT calculated UV-vis spectrum of DPP-T-C2C6C8 backbone with twisted ϕ_{T-T} and ϕ_{D-T} dihedral angles.

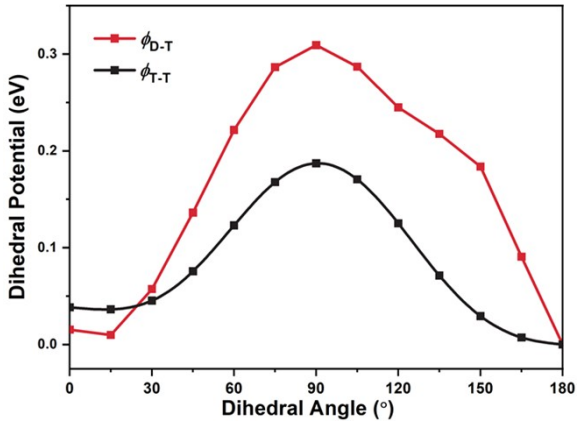

Figure S9. Dihedral potential for a DPP-based trimer.

ϕ_{T-T} and ϕ_{D-T} dihedral angles potential energy surfaces were calculated (**Figure S8**). The dihedral potential between DPP-thiophene units shows a sharper increase than the dihedral potential between thiophene-thiophene units when deviating coplanar conformations, which indicates the formation of oxygen-sulfur and oxygen-hydrogen interactions.[3] Such nonbonding interactions are expected to reduce the conformational disorder and promote the planar conformation.[4]

Table S1. Values calculated for the dihedral angles (in degrees) of DPP-based dimers.

	ϕ_{T-T}	ϕ_{D-T}
DPP-T-C2C6C8	171	162
DPP-T-C2C8C10	173	161
DPP-T-C2C10C12	179	158
DPP-T-C2C12C14	176	154

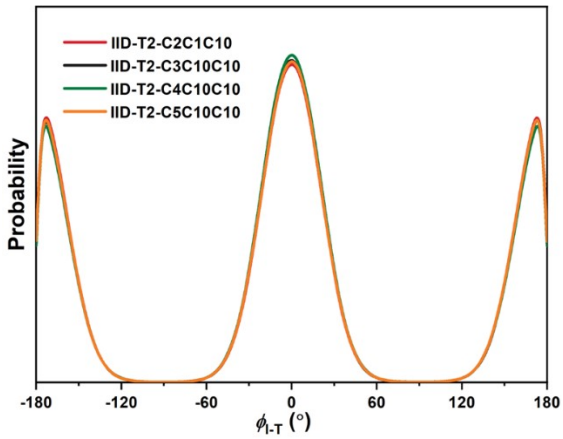

Figure S10. IID-thiophene dihedral angle distributions from AA-MD simulation.

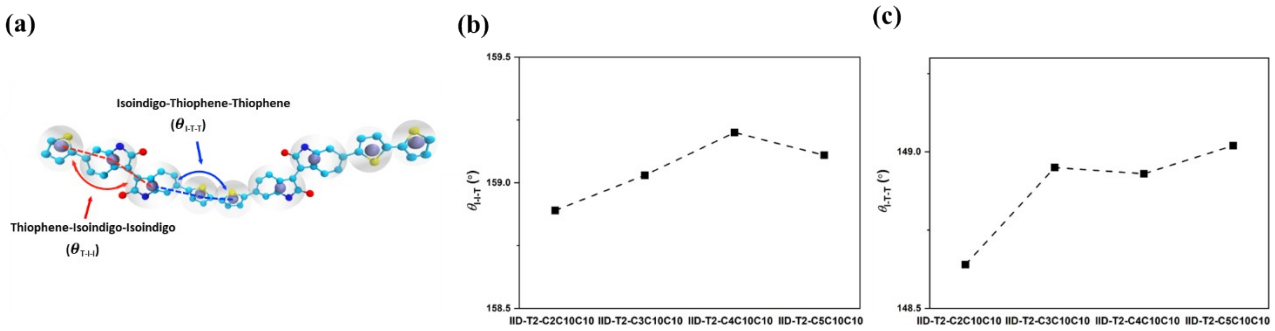

Figure S11. (a) Schematic definition of the bending angles. Grey beads denote the center of mass of each functional group. (b) Averaged bending angle between IID-thiophene rings for IID-based polymers. (c) Averaged bending angle between thiophene-thiophene rings for IID-based polymers.

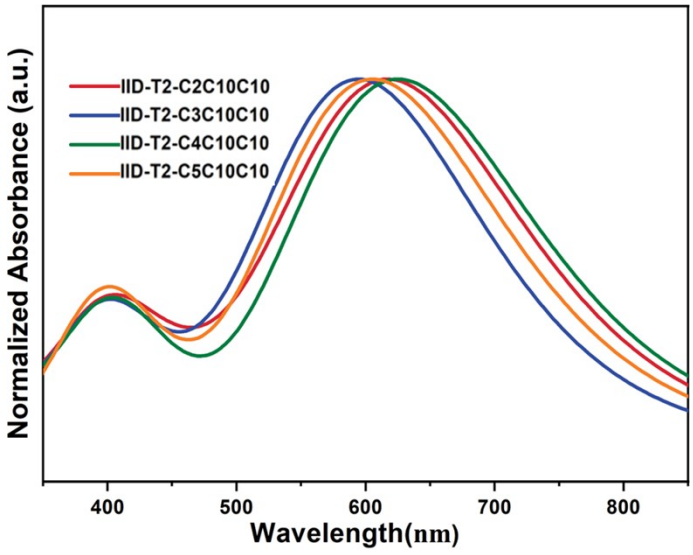

Figure S12. DFT calculated optical absorption based on the optimized ground-state electronic structure of IID trimers.

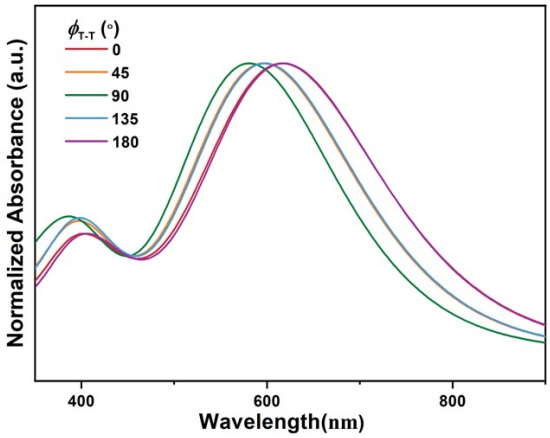

Figure S13. DFT calculated UV-vis spectrum of IID-T2-C2C10C10 backbone with twisted T-T dihedral angles.

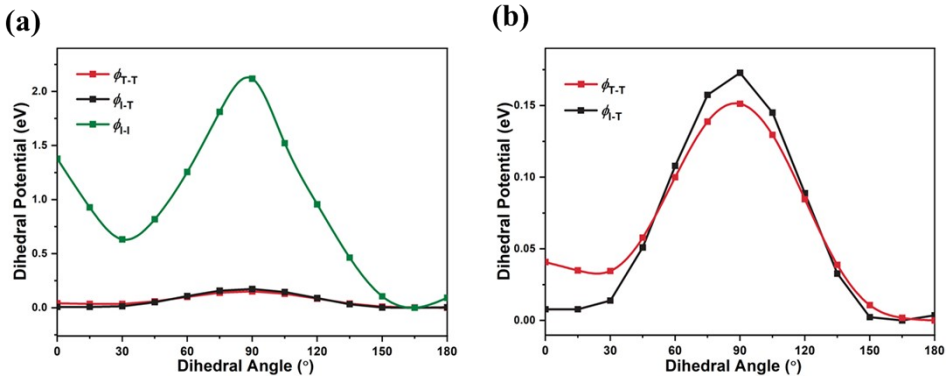

Figure S14. Dihedral potential for a IID-based trimer.

Dihedral potential between IID-thiophene units has global minimum at 0° and a local minimum at 170°. Dihedral potential between thiophene-thiophene units shows a global minimum at the trans state (180°) and a local minimum at the cis state (0°). ϕ_{T-T}, ϕ_{I-T}, and ϕ_{I-I} dihedral angle potential energy surfaces were also calculated (**Figure S12**). Our calculations show that intra-acceptor dihedral potential (ϕ_{I-I}) has a global minimum of around 165°. Thanks to the double-bond connection, as well the interactions between O atom in the electron-deficient lactam core and a proximal H atom, the rotational energy barrier inside the isoindigo unit is high. Such a high

rotational energy barrier is expected to reduce the conformational disorder and promote the planar conformation.

Table S2. Values calculated for the dihedral angles (in degrees).

	ϕ_{T-T}	ϕ_{I-T}	ϕ_{I-I}
IID-T2-C2C10C10	171	165	164
IID-T2-C3C10C10	163	163	160
IID-T2-C4C10C10	170	169	161
IID-T2-C5C10C10	164	166	163

References：

(1) Tsourtou, F. D.; Peristeras, L. D.; Apostolov, R.; Mavrantzas, V. G. Molecular Dynamics Simulation of Amorphous Poly (3- Hexylthiophene). *Macrolmolecules* **2020**, *53*, 7810–7824. https://doi.org/10.1021/acs.macromol.0c00454.

(2) Zhang, W.; Gomez, E. D.; Milner, S. T. Predicting Nematic Phases of Semiflexible Polymers. *Macromolecules* **2015**, *48* (5), 1454–1462. https://doi.org/10.1021/acs.macromol.5b00013.

(3) Jackson, N. E.; Savoie, B. M.; Kohlstedt, K. L.; Olvera, M.; Cruz, D.; Schatz, G. C.; Chen, L. X.; Ratner, M. A. Controlling Conformations of Conjugated Polymers and Small Molecules : The Role of Nonbonding Interactions. *J. Am. Chem. Soc.* **2013**, *135* (28), 10475–10483.

(4) Mikie, T.; Okamoto, K.; Iwasaki, Y.; Koganezawa, T.; Sumiya, M.; Okamoto, T.; Osaka, I. Naphthobispyrazine Bisimide: A Strong Acceptor Unit for Conjugated Polymers Enabling Highly Coplanar Backbone, Short Π–π Stacking, and High Electron Transport. *Chem. Mater.* **2022**, *34* (6), 2717–2729. https://doi.org/10.1021/acs.chemmater.1c04196.